

## Ferromagnetic resonance measurement using stroboscopic magneto-optical Kerr effect

Takahiro Moriyama, Seungha Yoon, and Robert D. McMichael

Citation: *Journal of Applied Physics* **117**, 213908 (2015); doi: 10.1063/1.4922126

View online: <http://dx.doi.org/10.1063/1.4922126>

View Table of Contents: <http://scitation.aip.org/content/aip/journal/jap/117/21?ver=pdfcov>

Published by the AIP Publishing

---

### Articles you may be interested in

[Development of microscopic magnetometer with reflective objective using magneto-optical Kerr effect](#)

*J. Appl. Phys.* **111**, 07E324 (2012); 10.1063/1.3675176

[Determination of the saturation magnetization of ion irradiated Py/Ta samples using polar magneto-optical Kerr effect and ferromagnetic resonance](#)

*Appl. Phys. Lett.* **96**, 022503 (2010); 10.1063/1.3291051

[Soft x-ray resonant magneto-optical Kerr effect as a depth-sensitive probe of magnetic heterogeneity: Its application to resolve helical spin structures using linear p polarization](#)

*J. Appl. Phys.* **96**, 7414 (2004); 10.1063/1.1806535

[A computational method of temperature characteristics of magneto-optical Kerr effect in amorphous TbFeCo films with a multilayered structure](#)

*J. Appl. Phys.* **93**, 5268 (2003); 10.1063/1.1565828

[Layer-resolved magnetometry of a magnetic bilayer using the magneto-optical Kerr effect with varying angle of incidence](#)

*J. Appl. Phys.* **85**, 4818 (1999); 10.1063/1.370492

---

Frustrated by old technology?      Is your AFM dead and can't be repaired?      Sick of bad customer support?



**It is time to upgrade your AFM**  
Minimum \$20,000 trade-in discount for purchases before August 31st

**Asylum Research is today's technology leader in AFM**

[dropmyoldAFM@oxinst.com](mailto:dropmyoldAFM@oxinst.com)

**OXFORD INSTRUMENTS**  
The Business of Science®

# Ferromagnetic resonance measurement using stroboscopic magneto-optical Kerr effect

Takahiro Moriyama,<sup>1,2</sup> Seungha Yoon,<sup>1,3</sup> and Robert D. McMichael<sup>1</sup>

<sup>1</sup>Center for Nanoscale Science and Technology, National Institute of Standards and Technology, Gaithersburg, Maryland 20899, USA

<sup>2</sup>Institute for Chemical Research, Kyoto University, Uji, Kyoto, Japan

<sup>3</sup>Maryland Nanocenter, University of Maryland, College Park, Maryland 20742, USA

(Received 17 April 2015; accepted 25 May 2015; published online 2 June 2015)

We have developed a novel ferromagnetic resonance (FMR) measurement technique using the magneto-optical Kerr effect. The measurement technique uses microwave-frequency, intensity-modulated light to stroboscopically measure the Kerr angle due to the magnetization precession. We demonstrate that this stroboscopic magneto-optical Kerr effect provides a frequency domain and phase sensitive FMR measurement. The measurement is sensitive enough to detect the precessing magnetization with the precession cone angle below  $1^\circ$ . © 2015 AIP Publishing LLC. [<http://dx.doi.org/10.1063/1.4922126>]

## INTRODUCTION

Ferromagnetic resonance (FMR) is an important technique for investigating both the static and dynamic properties of ferromagnets<sup>1–5</sup> and spintronic devices. For modern magnetic storage applications, such as hard disk drives (HDD) and magnetic random access memory (MRAM), FMR is especially helpful for characterizing magnetic anisotropy and damping in materials. In particular, the anisotropy is important for the thermal stability of the magnetic data bits and both the anisotropy and damping determine the writing current of spin-torque MRAM.<sup>6</sup>

The scaling of devices and magnetic recording bits to the nanometer scale also indirectly creates a need for higher frequency measurement. In nanomagnets, the effects of thermal agitation of the magnetization are increasingly significant, and to maintain stability of recorded information, high magnetic anisotropy materials are needed.<sup>7–10</sup> Since the ferromagnetic resonant frequency increases with the anisotropy field, pursuit of materials with higher thermal stability can create a need for resonant frequency measurements at frequencies over 100 GHz.<sup>11</sup>

Conventional FMR methods using commercially available connectors, waveguides, and cabling are generally limited in frequency range up to tens of gigahertz. For higher frequency electric circuits, the waveguides and connectors become significantly more expensive, and they have greater losses. For higher frequencies and shorter time scales, optical techniques provide opportunities to extend the frequency bandwidth to the terahertz regime. Time resolved magneto-optical Kerr effect (TR-MOKE) is one of such optical FMR techniques widely used for investigating magnetization dynamics.<sup>12</sup> TR-MOKE employs a femtosecond pulsed laser to excite the magnetization, and a weaker, delayed pulse to detect the magnetization state as a function of time delay after the pump pulse.

In this work, we have developed a hybrid magneto-optical/microwave technique that uses conventional microwave methods to excite magnetization precession, but optical

methods for detection. Previous hybrid measurement methods include continuous microwave excitation of the sample and optical detection using a fast photodetector<sup>13</sup> or a sophisticated heterodyne detection scheme.<sup>14</sup> Here, we take advantage of developments in fiber-optic telecommunication devices to create 1550 nm light that is amplitude modulated at the microwave frequency (RF), and we use this light to perform phase-sensitive stroboscopic measurements of the magnetization precession.

## EXPERIMENTAL

A schematic of our measurement setup is shown in Fig. 1. It is composed of two main parts: the RF circuitry to excite the magnetization dynamics and the optical “circuitry” to detect the magnetization dynamics. These two main parts are coupled

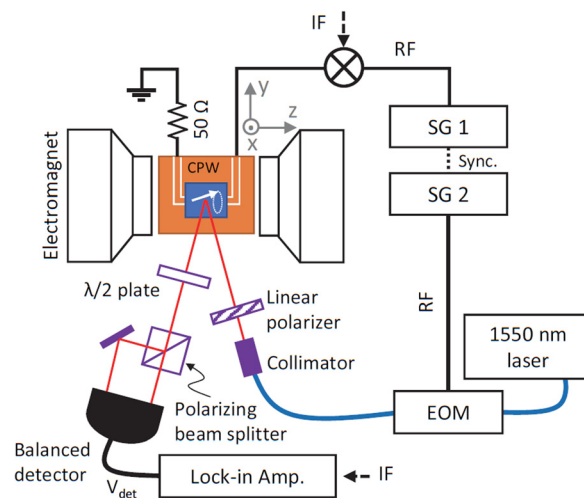


FIG. 1. Schematic of the measurement setup. Signal generator 1 (SG 1) feeds the RF current to the coplanar waveguide (CPW). Signal generator 2 (SG 2) feeds the RF current to the electro-optical modulator (EOM). Frequencies of SG 1 and SG 2 are synchronized. The electric circuitry, the optical fiber circuitry, and the light path in free space are drawn by the black, blue, and red lines, respectively.  $V_{det}$  is detected at the balanced detector as a result of the Kerr angle rotation.

by a pair of synchronized microwave signal generators, SG 1 and SG 2.<sup>15</sup>

The output of SG 1 is fed to a coplanar waveguide (CPW) for excitation of the magnetization in a 30 nm thick film of Fe<sub>18</sub>Co<sub>72</sub>B<sub>10</sub> (FeCoB), which was deposited on a 300 μm thick silicon substrate. The sample is glued onto the CPW with its film facing upward so that the laser is directly incident on the FeCoB film, and the CPW is placed between the poles of an electromagnet such that the static magnetic field is parallel to the sample plane. The RF current in the CPW creates a RF magnetic field orthogonal to the static magnetic field and mostly in the plane of the sample film. To improve signal-to-noise quality, the RF current is amplitude modulated at 10 kHz intermediate frequency (IF), and the signal from the photodetector is demodulated by the lock-in amplifier. This arrangement allows shot-noise-limited operation of the balanced detector.<sup>16</sup>

In the optical part of the setup, we use a linearly polarized telecommunications fiber laser (wavelength = 1550 nm) and electro-optical modulator (frequency bandwidth of 10 GHz) to create light with the same frequency as the RF current used for excitation. The modulator's microwave driving amplitude and DC offset are adjusted to achieve nearly full modulation of the light intensity, which we verify using a fast photodiode and microwave oscilloscope. The modulated laser light is then collimated in free space, and directed onto the sample at 20° away from the sample normal. The incident light is polarized and aligned by a three-paddle polarization controller in the fiber (not shown) and polarizer. The reflected light passes through a λ/2 wave plate and a polarizing beam splitter to be detected by a balanced detector. The λ/2 wave plate is adjusted to obtain a power ratio in the signal and the reference channels that is suitable for auto-balancing.

We record the voltage detected by the balanced detector,  $V_{det}$ , while sweeping the static magnetic field and maintaining a constant RF frequency. On resonance, the magnetization precession in the FeCoB creates a Kerr angle oscillation at the RF frequency. The oscillation in the Kerr angle and the modulation in the light intensity mix to produce a slowly varying (IF) voltage signal at the balanced detector, as will be shown below in a detailed derivation. We modulate the microwave power to the coplanar waveguide at 10 kHz, and we use a lock-in amplifier to perform phase-sensitive detection. This arrangement is necessary both because the auto-balance feature of the detector nulls low-frequency signals, and also because it allows us to measure in a frequency range where 1/f noise is not dominant.

## THEORY

FMR is well explained by the phenomenological Landau-Lifshitz-Gilbert equation.<sup>17,18</sup> We consider a soft magnetic film with magnetization  $M_s$  in a slowly varying applied field  $H \parallel \hat{z}$  and a microwave magnetic field  $H_{RF} = h_0 \cos(\omega t + \theta) \parallel \hat{y}$ . The phase  $\theta$  reflects the difference in effective path lengths for the microwave signal and optical signal reaching the sample. Near the ferromagnetic resonance condition given by

$$\omega_0 = \gamma \sqrt{H_0(H_0 + M_s)}. \quad (1)$$

The out-of-plane component of the magnetization induced by the RF magnetic field is

$$\delta m_x = h[\chi'_{xy} \cos(\omega t + \theta) + \chi''_{xy} \sin(\omega t + \theta)]. \quad (2)$$

Here, the off-diagonal component of the susceptibility tensor is separated into a symmetric real part,  $\chi'$  and an antisymmetric imaginary part,  $\chi''$

$$\begin{aligned} \chi' &= \frac{M_s \omega / \gamma}{2(2H + M_s)} \frac{\delta H}{[(H - H_0)^2 + \delta H^2]}, \\ \chi'' &= \frac{M_s \omega / \gamma}{2(2H + M_s)} \frac{(H - H_0)}{[(H - H_0)^2 + \delta H^2]}, \end{aligned} \quad (3)$$

where  $H_0$  is the resonance field, the half-linewidth is  $\delta H = \alpha \omega_0 / \gamma$ , where  $\gamma$  is the gyromagnetic ratio and  $\alpha$  is the phenomenological Gilbert damping parameter.

The out-of-plane component of the magnetization is measured via the magneto-optical Kerr effect. Upon reflection from the sample, the polarization of the light is rotated by an angle  $\delta\varphi$ , which is proportional to  $\delta m_x$  by  $\delta\varphi = \Phi_k \delta m_x / M_s$ , where  $\Phi_k$  is the Kerr rotation angle. For small polarization angle rotations, the auto-balanced detector yields a voltage that is the product of a gain factor  $A$ , the total incident power on the detectors,  $P_0$ , and the polarization angle fluctuation

$$V(t) = A P_0(t) \delta\varphi(t). \quad (4)$$

The light power has a time dependence that is produced by the electro-optic modulator

$$P(t) = P_0 \frac{[1 + \cos(\omega t)]}{2}. \quad (5)$$

Because the polarization angle and the light intensity both contain components that oscillate at frequency  $\omega$ , the product of the light intensity and the polarization angle yields a slowly varying term and also terms that oscillate at frequencies  $\omega$  and  $2\omega$ . As the photodetector frequency response is limited to 100 kHz, only the slowly varying term is important

$$V = \frac{\Phi_K}{2M_s} A P_0 h_0 [\chi' \cos(\theta) + \chi'' \sin(\theta)]. \quad (6)$$

The detected voltage is therefore a combination of the real and imaginary parts of the susceptibility that depends on the relative phase between the microwave field and the intensity of the incident light.

## RESULTS

Figure 2 shows the spectra of the detector output voltage,  $V_{det}$  as a function of the external field. The spectra exhibit features at magnetic fields that shift to higher field as the RF frequency increases. We fit these features using

$$V_{det}(H) = \Gamma [S(H) \cos \theta + A(H) \sin \theta], \quad (7)$$

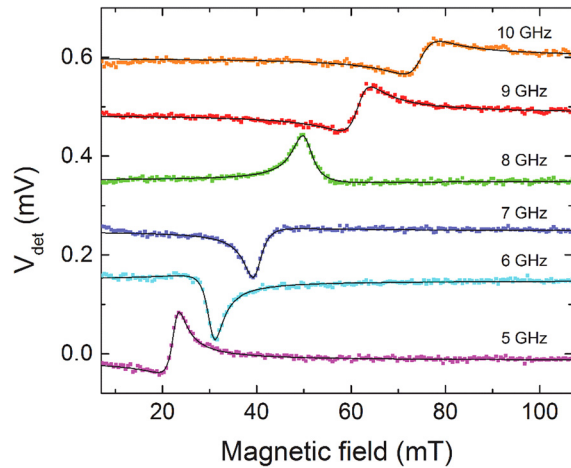


FIG. 2. The voltage detected by the balanced detector ( $V_{det}$ ) as a function of the external magnetic field. The applied frequency is varied from 5 GHz to 10 GHz. The dots are the experimental data, and the black curves are the fits to Eq. (7). The spectra are offset vertically for clarity.

where

$$\Gamma = \frac{AP_0\Phi_k h_0}{4\delta H} \frac{\omega/\gamma}{(2H + M_s)}. \quad (8)$$

The functions

$$S(H) = \frac{\delta H^2}{[(H - H_0)^2 + \delta H^2]}, \quad (9)$$

$$A(H) = \frac{[(H - H_0)\delta H]}{[(H - H_0)^2 + \delta H^2]} \quad (10)$$

are a symmetric Lorentzian and antisymmetric Lorentzian, respectively, following the form of Eq. (3). The lines in Fig. 2 demonstrate that Eq. (7) describes that data well, and the fits yield reasonable values for  $H_0$ ,  $\delta H$ ,  $\theta$ , and  $\Gamma$ .

The resonance field  $H_0$  and the linewidth  $\sigma$  obtained from the fits of the spectra are summarized in Fig. 3. The saturation magnetization of  $\mu_0 M_s = 1.6 \pm 0.1$  T was estimated from the plot in Fig. 3(a) by fitting using Eq. (2). In this fit, we assumed that the gyromagnetic ratio is  $\gamma \approx 28$  GHz/T. For applied fields  $H \ll M_s$ , as in this experiment, the values of  $\gamma$  and  $M_s$  are difficult to fit separately, but among the transition metals,  $\gamma$  typically varies by only 5%. Therefore, we have incorporated this variability of  $\gamma$  in our uncertainty estimate for  $M_s$ .

The Gilbert damping was also estimated to be  $\alpha = 0.0095 \pm 0.0004$  by the plot in Fig. 3(b) using  $\delta H = \alpha\omega_0/\gamma$ . Uncertainties reported here represent one standard deviation of the fit. The fit values of  $\mu_0 M_s$  and  $\alpha$  are in reasonable agreement with other reports.<sup>19</sup> The other fitting parameter  $\Gamma$  is also useful for evaluating the measurement sensitivity with respect to the magnitude of magnetization precession. For instance, at 10 GHz we obtained  $\Gamma = -65 \pm 2 \mu\text{V}$ . With  $A = 200$  V/mW defined by the balanced detector,  $P_0 = 1$  mW,  $\delta H = 3.73$  mT, and assuming  $\Phi_k$  to be on the order of  $10^{-3}$  rad, we estimate the parameter  $h_0$  to be on the order of 0.02 mT, which yields the precession cone angle in the film-normal direction  $\varepsilon = \sin^{-1}|\delta m_x| \approx 1^\circ$ . The estimation of  $h_0$  from the signal amplitude is in order-of-magnitude agreement with the value  $h_0 = 0.017$  mT calculated based on the RF

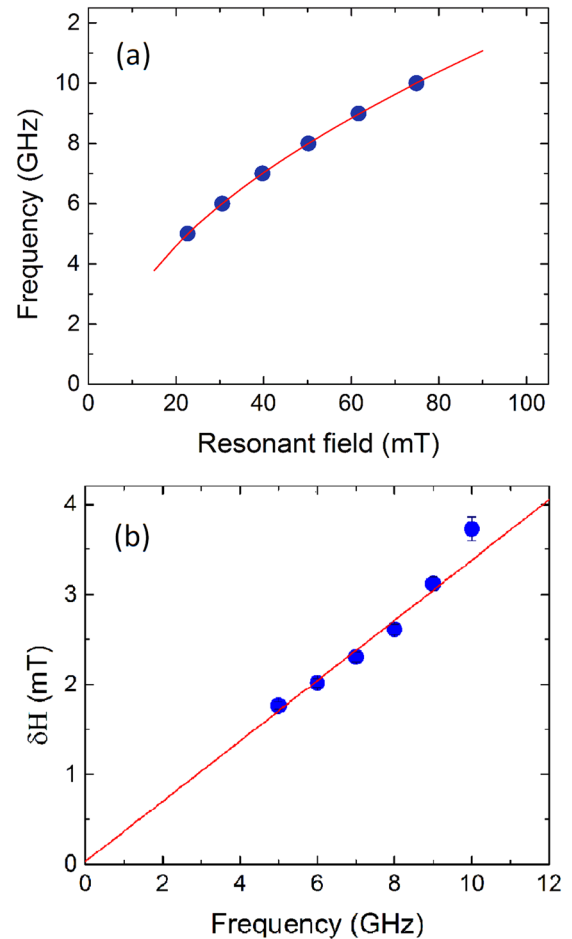


FIG. 3. (a) The RF frequency as a function of the resonant magnetic field. Error bars are smaller than most of the data markers. The red curve is a fit to Eq. (1). (b) The linewidth  $\delta H$  as a function of the resonant frequency. The experimental data are fit to  $\delta H = \alpha\omega_0/\gamma$  to obtain the Gilbert damping parameter. The error-bars represent the standard deviation of the fit.

power ( $=31$  mW) applied to the CPW. Since the magnetization precession is elliptical due to the strong demagnetizing field, the cone angle in the in-plane direction is generally greater and is estimated to be  $\sim 5^\circ$ . Our FMR signals predominantly come from the film normal component of the precession  $\delta m_x$  due to our optical configuration, which is sensitive to the polar Kerr effect. We emphasize that based on our observed noise level, this measurement is sensitive enough to detect magnetization precession angles less than  $1^\circ$ .

Since Eq. (7) suggests that the variation in the spectrum shapes shown in Fig. 2 is already indicative of phase sensitive detection, we performed control measurements to demonstrate the phase sensitivity in our stroboscopic technique. We apply a microwave field at a constant RF frequency of 5 GHz into both the electro-optical modulator and CPW. Then, the phase of the RF current on the CPW is controlled by the phase shifter in SG 1. In this way, the magnetization precession phase relative to the laser pulse phase can be deliberately controlled. As shown in Fig. 4, the stroboscopic FMR spectra show a linear phase change from the symmetric to antisymmetric Lorentzian, when the phase delay of SG 1 varies from  $0^\circ$  to  $360^\circ$ . The fitted phase angle of the Kerr signal  $\theta$  increases at the same rate as the phase delay made in

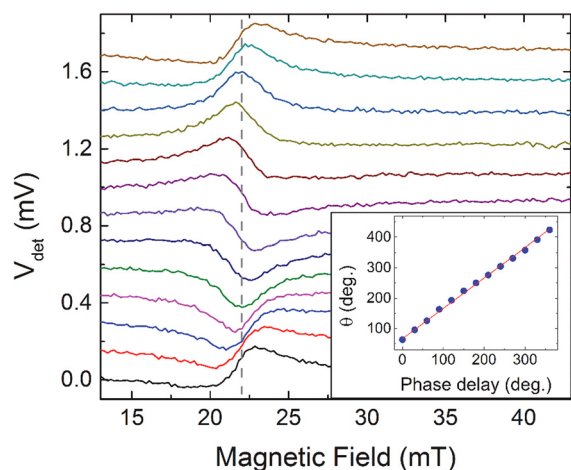


FIG. 4. A series of  $V_{det}$  spectra with various phase delays set at SG 1. The spectra are offset vertically by an equal amount for clarity. From the bottom-most spectrum to the top, the phase delay is increased in increments of  $30^\circ$  from  $0^\circ$  to  $360^\circ$ . The vertical dotted line indicates the position of the resonant field. The inset shows  $\theta$  obtained from Eq. (7) as a function of the phase delay set at SG 1. The red line, included for comparison, has a slope of 1.

SG 1 (inset in Fig. 4), showing that our stroboscopic measurement is sensitive to the relative FMR phase variations. The fit  $\theta$  values have standard deviations less than  $1.0^\circ$ . This phase sensitive capability would be especially useful for investigating the magnetization dynamics involving a small perturbation due to spin Hall torque and spin orbit torques.<sup>20–22</sup>

## CONCLUSION

This demonstration of stroboscopic detection is a step on the path to an all-optical FMR measurement technique, analogous to the optically driven TR-MOKE, but where the oscillation of the laser intensity (requiring much higher intensity than we used in this work) would simultaneously excite continuous magnetization precession via heating and or demagnetization, and also would detect precession via the stroboscopic magneto-optical Kerr effect. For high-frequency operation, it would be desirable to eliminate the need for frequency-limiting microwave components, such as signal generators, modulators, and waveguides. Instead, we anticipate that such an all optical system would rely on current developments in lasers with microwave and millimeter wave repetition rates to replace the electro-optical modulator and microwave signal generator.<sup>23–27</sup>

In summary, we have developed a new FMR measurement technique using stroboscopic magneto-optical Kerr effect and we have demonstrated the operational principle of this measurement. In the resonance condition, oscillations in the Kerr angle and in the light pulses mix to produce a slowly varying resonance voltage signal. The FMR spectral peak was characterized by a superposition of a symmetric Lorentzian and an antisymmetric Lorentzian. From the peak shape, we were able to estimate the oscillation phase of the magnetization precession with respect to the oscillation of

the light intensity, proving that this novel measurement technique is phase sensitive. We suggest that the same operation principle could be used to extend the measurement bandwidth up to the terahertz regime for ultrafast dynamics measurements.

## ACKNOWLEDGMENTS

T.M. was supported by the Kyoto University Foundation and Grant-in-Aid for Young Scientists (B) from Japan Society for the Promotion of Science. Dr. Yoon acknowledges support under the Cooperative Research Agreement between the University of Maryland and the National Institute of Standards and Technology Center for Nanoscale Science and Technology, Award No. 70NANB10H193, through the University of Maryland.

- <sup>1</sup>C. Kittel, *Phys. Rev.* **73**, 155 (1948).
- <sup>2</sup>G. Yu, Z. Wang, M. Abolfath-Beygi, C. He, X. Li, K. L. Wong, P. Nordeen, H. Wu, G. P. Carman, X. Han, I. A. Alhomoudi, P. K. Amiri, and K. L. Wang, *Appl. Phys. Lett.* **106**, 072402 (2015).
- <sup>3</sup>X. Liu, Y. Sasaki, and J. K. Furdyna, *Phys. Rev. B* **67**, 205204 (2003).
- <sup>4</sup>P. G. Barreto, M. A. Sousa, F. Pelegrini, W. Alayo, F. J. Litterst, and E. Baggio-Saitovitch, *Appl. Phys. Lett.* **104**, 202403 (2014).
- <sup>5</sup>E. Montoya, T. McKinnon, A. Zamani, E. Girt, and B. Heinrich, *J. Magn. Magn. Mater.* **356**, 12 (2014).
- <sup>6</sup>J. Z. Sun, *Phys. Rev. B* **62**, 570 (2000).
- <sup>7</sup>G. Jan, Y.-J. Wang, T. Moriyama, Y.-J. Lee, M. Lin, T. Zhong, R.-Y. Tong, T. Torng, and P.-K. Wang, *Appl. Phys. Exp.* **5**, 093008 (2012).
- <sup>8</sup>M. Nakayama, T. Kai, N. Shimomura, M. Amano, E. Kitagawa, T. Nagase, M. Yoshikawa, T. Kishi, S. Ikegawa, and H. Yoda, *J. Appl. Phys.* **103**, 07A710 (2008).
- <sup>9</sup>D. Weller and A. Moser, *IEEE Trans. Magn.* **35**, 4423 (1999).
- <sup>10</sup>M. H. Kryder, E. C. Gage, T. W. McDaniel, W. A. Challener, R. E. Rottmayer, G. Ju, Y.-T. Hsia, and M. F. Erden, *Proc. IEEE* **96**, 1810 (2008).
- <sup>11</sup>S. Mizukami, A. Sakuma, T. Kubota, Y. Kondo, A. Sugihara, and T. Miyazaki, *Appl. Phys. Lett.* **103**, 142405 (2013).
- <sup>12</sup>W. K. Hiebert, A. Stankiewicz, and M. R. Freeman, *Phys. Rev. Lett.* **79**, 1134 (1997).
- <sup>13</sup>H. T. Nembach, J. M. Shaw, C. T. Boone, and T. J. Silva, *Phys. Rev. Lett.* **110**, 117201 (2013).
- <sup>14</sup>J. M. Shaw, T. J. Silva, M. L. Schneider, and R. D. McMichael, *Phys. Rev. B* **79**, 184404 (2009).
- <sup>15</sup>In principle, one signal generator with a microwave splitter, phase shifter, and microwave amplifier (if necessary) would be sufficient to demonstrate the present measurement.
- <sup>16</sup>P. C. D. Hobbs, *Appl. Opt.* **36**, 903 (1997).
- <sup>17</sup>L. D. Landau and E. M. Lifshitz, *Phys. Z. Sowietunion* **8**, 153 (1935).
- <sup>18</sup>T. L. Gilbert, *Phys. Rev.* **100**, 1243 (1955).
- <sup>19</sup>S. Iihama, S. Mizukami, H. Naganuma, M. Oogane, Y. Ando, and T. Miyazaki, *Phys. Rev. B* **89**, 174416 (2014).
- <sup>20</sup>J. C. Sankey, Y.-T. Cui, J. Z. Sun, J. C. Slonczewski, R. A. Buhrman, and D. C. Ralph, *Nat. Phys.* **4**, 67 (2008).
- <sup>21</sup>H. Kubota, A. Fukushima, K. Yakushiji, T. Nagahama, S. Yuasa, K. Ando, H. Maehara, Y. Nagamine, K. Tsunekawa, D. D. Djayaprawira, N. Watanabe, and Y. Suzuki, *Nat. Phys.* **4**, 37 (2008).
- <sup>22</sup>L. Liu, T. Moriyama, D. C. Ralph, and R. A. Buhrman, *Phys. Rev. Lett.* **106**, 036601 (2011).
- <sup>23</sup>P. Del'Haye, A. Schliesser, O. Arcizet, T. Wilken, R. Holzwarth, and T. J. Kippenberg, *Nature* **450**, 1214 (2007).
- <sup>24</sup>T. J. Kippenberg, R. Holzwarth, and S. A. Diddams, *Science* **332**, 555 (2011).
- <sup>25</sup>A. Martinez and S. Yamashita, *Appl. Phys. Lett.* **101**, 041118 (2012).
- <sup>26</sup>F. Li and A. S. Helmy, *Opt. Lett.* **38**, 4542 (2013).
- <sup>27</sup>A. Haboucha, W. Zhang, T. Li, M. Lours, A. N. Luiten, Y. Le Coq, and G. Santarelli, *Opt. Lett.* **36**, 3654 (2011).